Chapter 2 : LITERATURE REVIEW

2.1 Introduction

When explosive detonates in the blast hole, a particular amount of energy is released in the surroundings forming compressional stress and gases at high pressure and temperature. These rapid exothermic oxidation and expansion occurs around the blast holes.This sudden impact causes dynamic loading on the surrounding rockmass resulting in the crushing of rocks, radial cracking around the holes, and the refelection of waves upon incidence on free face. After the explosion, the released stress energy propagates into the ground as a vibration or seismic wave radially outward in all directions and covers some distance from the blast site. This distance mainly depends on the intensity of the released energy. The intensity of the ground vibration depends mainly on the controllable parameters like a burden, spacing, the maximum charge per delay, dimensions of blast holes, etc. and uncontrollable parameters like geology, physico-mechanical properties of the blast site. Quantification of the ground vibrations has traversed much and has settled for peak particle velocity and frequency after experimenting with displacement and acceleration. Now, the intensity of ground vibration is generally expressed by peak particle velocity and dominant frequency at a particular site (Duvall and Wilbur 1959; Stagg et al. 1980; Statura et al. 1984; Dowding 1985; Singh and Sngh, 2005; Khandelwal and Singh, 2007). During the last few decades, many scientists and researchers developed different empirical models and standards for the damage criteria for their specific purposes to assess the ground vibration levels and its impacts on nearby structures. (Duvall et al. 1962; Elevli and Ercan, 2010). Nowadays, some approaches and algorithms are being used to evaluate, correlate, and predict blast-induced ground vibrations and its impacts. The main objective of this literature is to describe and elaborate on different types of parameters and factors that affect the ground vibrations and consequent damages to the nearby surrounding structures.

2.2 Blast-induced Ground Vibration (BIGV)

The blasting is the after-effect of explosions planned and designed in mines and quarries. Blasting produces desirable energy in rock mass breakage and its displacement, whereas waste energy in the form of ground vibration, air overpressure, and noises. These blast-induced energies (BIE) also cause damage, accidental hazard, financial loss, and discomfort to the people living nearby. The distribution of the blast-induced energy is shown in Figure 2.1. The ground vibration covers the major part of the blast-induced waste energy. It propagates through the earth's surface in the form of various waves. The magnitude of vibration decreases with increasing the distance from the source. The parcel of mechanically induced energy travels into the earth's surface through the oscillation of particles. This energy is transferred from one particle to another by hitting and comes at rest. Oscillatory motion of particles by transferring energy creates the movement in the form of "vibration" or "shaking" of the ground surface, and this phenomenon is called ground vibration. The blast-induced ground vibration is an undesirable activity in mines as well as quarries, and the ground vibration and seismic energy are usually described as a time-varying displacement, velocity, and acceleration of a particle in the ground (Siskind, 1980). Several other incidents produce ground vibration at different levels by natural sources like tectonic activity, volcanic activity, and artificial sources like traffic, pile driving, sonic boom, etc. The earthquake produces long-durational and low-frequency events, while the blast-induced ground vibration produces short durational and high-frequency events. Both possess the potential damage to the structures (Arsenen, 2003).

The trend towards larger blasts using many delay intervals in many blocks leads to the overall lengthening of blast cycle duration and, consequently, the enhancement of seismic effects to structures to be protected. The total time of blast duration should be reduced by optimally selected delay intervals and the number of delay groups (Arseven, 2003).

According to **Atlas (1987),** ground motion dissipation in rock is attributed to three mechanisms:

- Viscous damping ground vibrations are more pronounced on higher frequencies and accompanied by a trend to lower ground vibration frequencies with increasing distance from a blast.
- The seismic wave's solid friction energy absorption is greater for rock for courser grain structures and extensive porosity.
- Ground vibrations are scattered and reflected from the rock's boundary discontinuities and stratum inhomogeneities. Interactions between reflected pulses are typically accompanied by a tendency to attenuate lower ground vibration frequencies (Atlas, 1987).

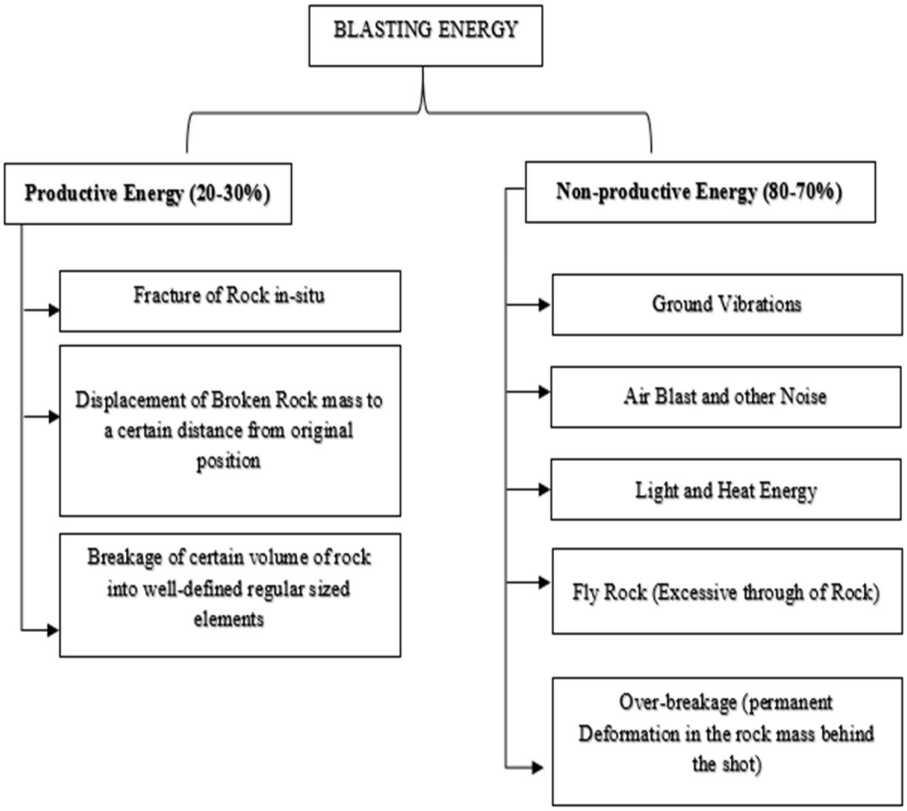

Figure 2.1 Distribution of blast-induced energy.

2.2.1 Mechanism of ground vibration

Due to the abrupt acceleration of rock mass and the build-up of gas pressure on the blast hole wall, intense dynamic stress energy was released surrounding the blast hole during the explosion of explosives within the blast hole. The stress-energy is dissipated into the surrounding rock mass that builds up motion in the ground, as shown in Figure 2.2. The strain

energy level exceeds the elastic limit of the rock mass, which causes the fragmentation with different breakage mechanisms such as; crushing of rock, radial cracking around blast hole into the rock mass, and reflection breakage in the free face as a back breakage. If no permanent deformation occurs into the rock mass, the strain energy waves propagate through the ground as elastic waves. The whole region beyond the fragmentation zone is known as the elastic zone. The propagating waves in this zone are seismic waves or ground vibrations and the behavior of elastic zone is visco-elastic. The seismic waves or ground waves move concentrically outward in all directions from the blast site, and the intensity of the ground wave decreases with increasing distance from the blast site. The excessive amount of explosives produce a high intensity of the ground vibrations causing damage to natural and artificial structures (Kutter and Fairhurst, 1971) .

Kutter and Fairhurst (1971) indicated three zones of varying destruction and deformation around the explosion, as shown in Figure 2.3. These zones are:

- The strong shock zone (hydrodynamic zone)
- The non-linear zone, and
- The elastic zone.

Olofsson (1988) revealed as the burden begins to move, high compressive stresses within the rock begin to unload and generate more tensile stresses, which complete the fragmentation process. Generally, the combined effects of shock and gas energies of an explosive cause the rock fracture during blasting and gas energy plays a relatively higher role during rock fragmentation depending upon the energy partitioning characteristics of the explosive. In the absence of free faces, the shock energy remaining after rock fracturing during the blast travels as seismic waves in the ground (Singh, 1999). The mechanical energy is converted into electrical signals after passing through the instruments and give digital output, as shown in Figure 2.4.

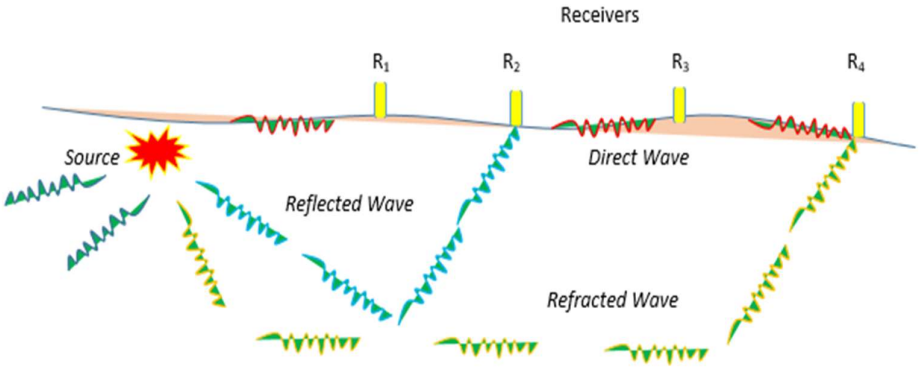

Figure 2.2 Propagation of various seismic waves (Kumar et al. 2021)

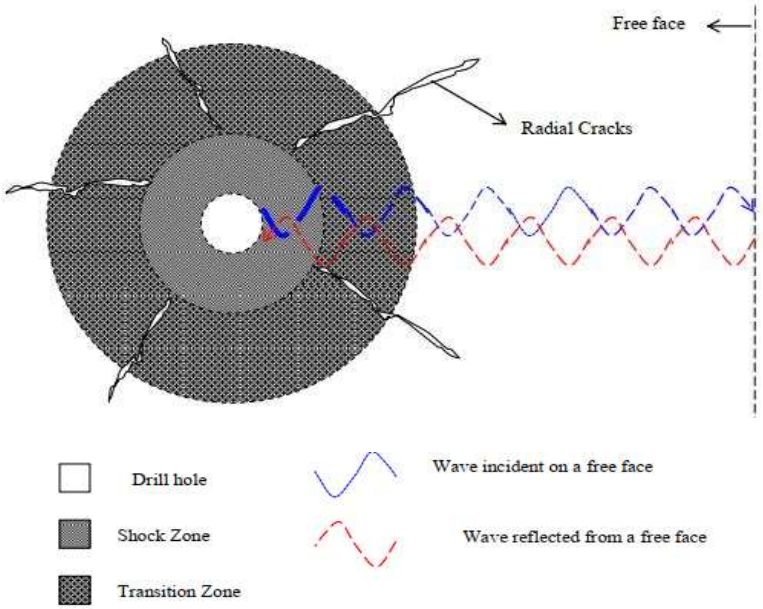

Figure 2.3 After effect of explosion around blast hole (Dowding and Aimone, 1992).

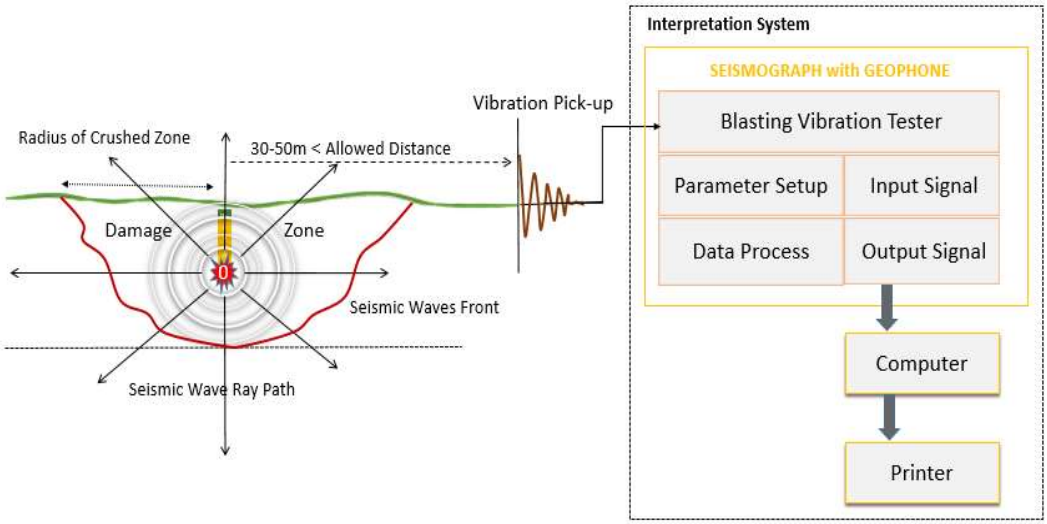

Figure 2.4 Conversion of mechanical energy into an electrical signal

2.3 Seismic Waves

Interactions between the propagating media and the vibrations give rise to several waves. The main wave types can be divided into body waves and surface waves (Dowding, 1985).

2.3.1 Body Wave

2.3.1.1 Primary Wave (P-wave)

Compressional waves are also known as the longitudinal, primary or P-waves of earthquake seismology, are propagated by compressional and dilatational uniaxial strains in the direction of wave propagation, as shown in Figure 2.5. Particle motion associated with the passage of a compressional wave involves oscillation, about a fixed point, in the direction of wave propagation (Bolt, 1982).

2.3.1.2 Secondary Wave (S-wave)

Shear waves (the transverse, secondary or S-waves of earthquake seismology) propagate by a pure shear strain in a direction perpendicular to the direction of wave travel, as shown in figure 2.6. Individual particle motions involve oscillation, about a fixed point, in a plane at right angles to the direction of wave propagation (Bolt, 1982).

2.3.2 Surface Wave

2.3.2.1 Rayleigh Wave

Rayleigh waves propagate along a free surface, or the boundary between two different solid media, the associated particle motions being elliptical in a plane perpendicular to the surface and containing the direction of propagation as shown in Figure 2.7. The orbital particle motion is the opposite of the circular particle motion associated with an oscillatory water wave and is described as the retrograde motion of waves (Bolt, 1982).

2.3.2.2 Love Wave

Love waves are polarized shear waves with a particle motion parallel to the free surface and perpendicular to the direction of wave propagation, as shown in Figure 2.8. The velocity of Love waves is intermediate between the shear wave velocity of the surface layer and that of deeper layers, and Love waves are inherently dispersive (Bolt, 1982).

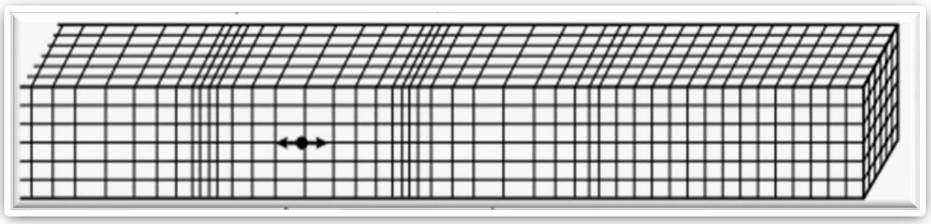

Figure 2.5 Longitudinal wave propagation (Bolt, 1982)

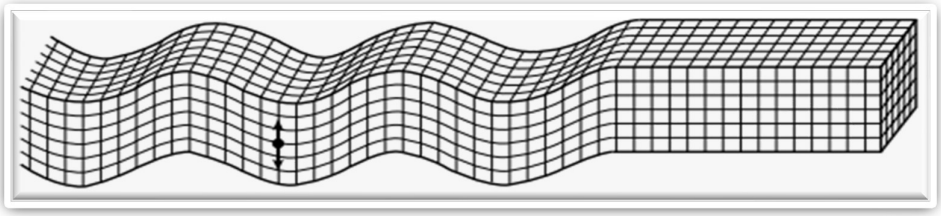

Figure 2.6 Shear wave propagation (Bolt, 1982)

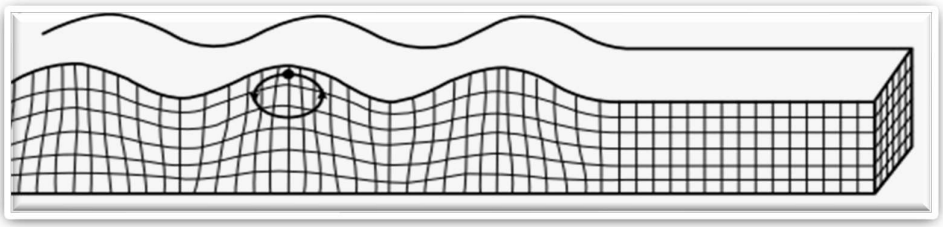

Figure 2.7 Rayleigh wave propagation (Bolt, 1982)

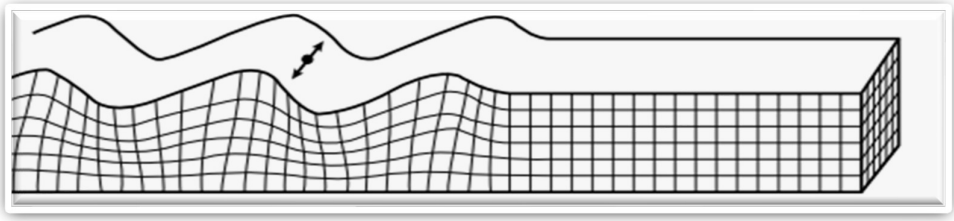

Figure 2.8 Love wave propagation (Bolt, 1982)

2.4 Seismic Wave Attenuation

Seismic attenuation is an intrinsic property of rocks, causing energy dissipation as seismic waves propagate through the subsurface. It results in the decay of amplitude of the seismic waves. Attenuation is related to velocity dispersion (Batzle et al. 2005). The energy of the seismic wave is conserved if it travels through a perfectly elastic medium. Propagating seismic waves lose energy due to geometrical, anelastic, and scattering attenuation (Durek and Goran, 1996).

2.4.1 Geometrical Attenuation

The most critical reduction is due to geometric attenuation. Consider the seismic body waves generated by a seismic source on the surface of a uniform half-space. If there is no energy loss due to friction, the energy (E_b) in the wavefront at a distance x from its source is distributed over the surface of a hemisphere with an area of $2\pi x^2$. The intensity (or energy density, I_b) of the body waves is the energy per unit area of the wavefront, and at a distance, x is given by Equation (2.1).

$$I_b = E_b / 2\pi x^2 \quad (2.1)$$

The surface wave is constricted to spread out laterally, and disturbance affects the free surface and extends downwards into the medium to a depth d, which we can consider constant for a given wave. When the wavefront of a surface wave reaches a distance x from the source, the initial energy (Es) is distributed over a circular cylindrical surface with an area of $2\pi xd$. At a distance x from its origin, the intensity of the surface wave is given by Equation (2.2).

$$I_S = E_S / 2\pi xd \quad (2.2)$$

These equations show that the decrease in intensity of body waves is proportional to $1/x^2$ while the decline in surface wave intensity is proportional to $1/x$. Amplitude attenuations of body waves and surface waves are proportional to $1/x$ and $1/x^{0.5}$, respectively, shown in Figure 2.9. The seismic body waves are attenuated more rapidly than surface waves with

increasing distance from the source. These equations show that the decrease in intensity of body waves is proportional to $1/x^2$ while the decline in surface wave intensity is proportional to $1/x$ (Durek and Goran, 1996).

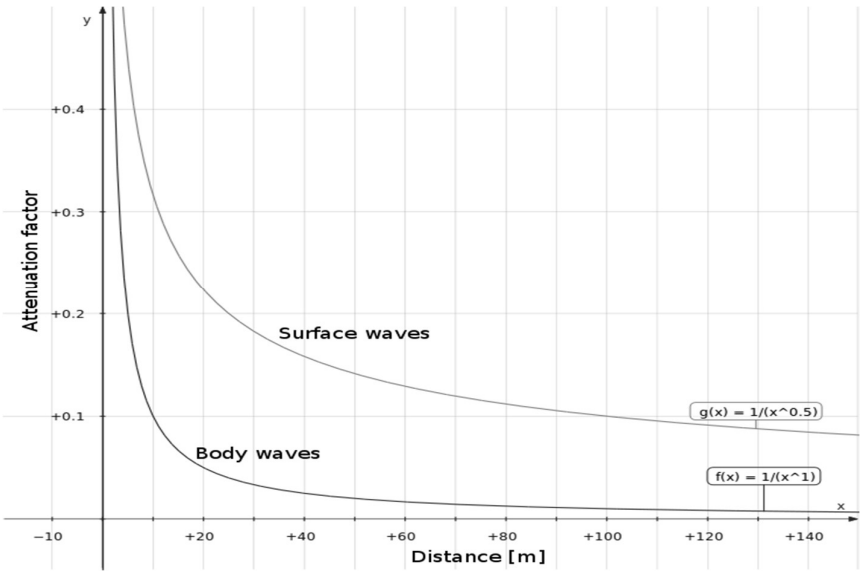

Figure 2.9 Geometrical attenuation of seismic wave (Durek and Goran, 1996).

2.4.2 Anelastic Attenuation

Another reason for attenuation is energy absorption due to imperfect elastic properties. Suppose the particles of a medium do not react perfectly elastically with their neighbors. In this case, several parts of the energy of the seismic waves are lost due to frictions and heating instead of the energy being transferred through the medium. This type of attenuation of the seismic wave is referred to as anelastic damping, as shown in Figure 2.10. A parameter describes the damping of seismic waves called the quality factor (Q), a concept borrowed from electric circuit theory. It represents the performance of an oscillatory circuit, as shown in Figure 2.3. The damped amplitude of a seismic wave at a distance x from its source. Another factor affects seismic wave amplitude and seismic wave energy loss due to anelastic attenuation by internal friction during wave propagation (Shapiro and Kneib, 1993).

Knopoff (1964) reviewed the literature on seismic wave attenuation and discussed the phenomenological approach. The seismic wave attenuation appears linear in the rock mass

and the earth interior. As measured in the laboratory, the internal friction of rocks is roughly independent of frequency 1 to 10^6 Hz, higher by orders of magnitude or more in poly-crystals than in single crystals, and is reasonable for very little dispersion, if any. Seismic experiments on soils, sandstone, and shale indicate that the internal friction is independent of frequency from 100 to 1000Hz. Observation of earthquake-induced seismic waves suggests more secondary wave attenuation than primary wave attenuation.

Gordon and Nelson (1966) have reviewed some possible attenuation mechanisms and emphasized the importance of frequency-dependent and thermally activated processes. They rank viscous grain-boundary damping, stress-induced order, and dislocation damping as the most probable source of seismic wave attenuation.

$$A = A_0 e^{-\pi x/Q\lambda} = A_0 e^{-x/\alpha} \quad (2.3)$$

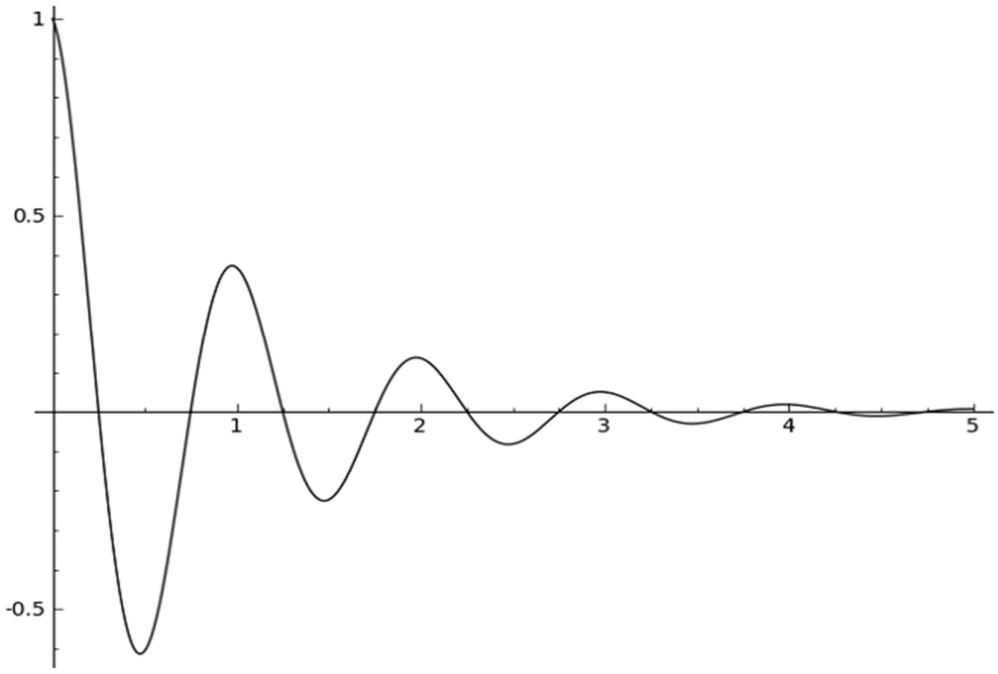

Figure 2.10 Anelastic loss of seismic wave (Durek and Goran, 1996).

2.5 Factors Affecting Ground Vibration

The blast-induced ground vibration is influenced by many factors such as;

- Geological condition
- Physical properties of rock mass
- Lithology of rock
- Types of rock

2.6 Blast Design Geometry

This is meant to be a toolbox for blast design in conventional rock quarrying and opencast mines. This write-up is not intended to give straight answers to the blast design parameters, as every quarry is unique. However, the general relationship among the blast design parameters, explosives parameters, geology, blastability, and explosives parameters will be applicable. The estimation model is an excellent tool for planning test blasts and experiments and adjustments of the blast design when this is necessary for optimizing the quarry production line as time progresses, as shown in Figure 2.11. High accuracy throughout the blasting process is fundamental for achieving an accurate blast result. Various points as success criteria are following:

- Planning
- Surveying and marking of holes
- Adjustment of drilling pattern
- Adjustment of specific charge
- Delay times and initiation pattern
- Accurate drilling
- Properly selected stemming material
- Control, documentation and supervision of the work

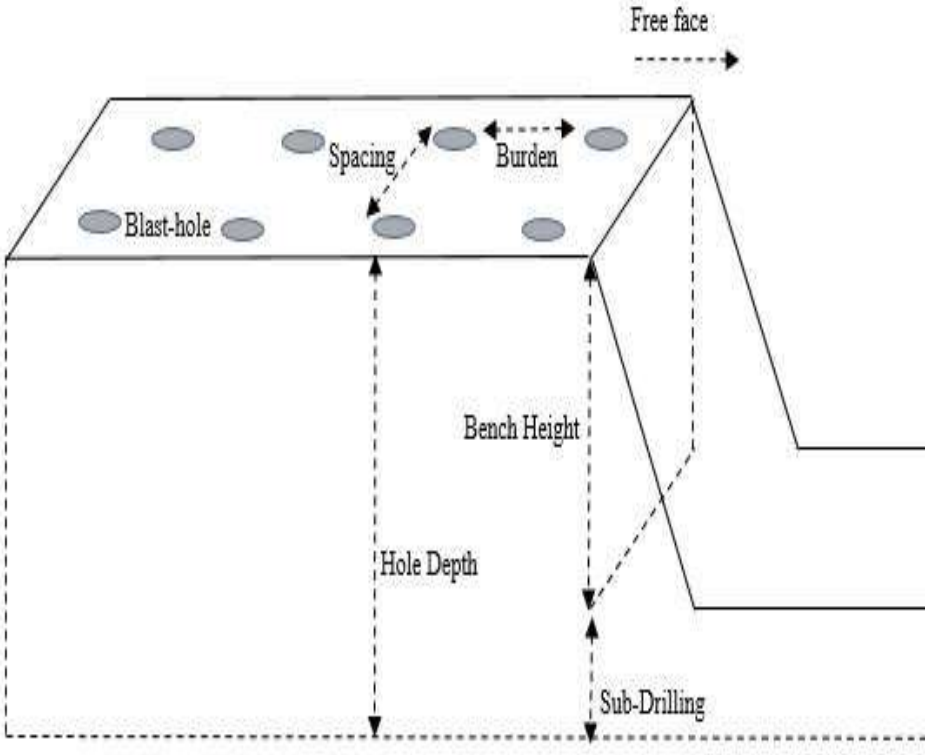

Figure 2.11 Geometry of blasting patch

2.6.1 Burden

The burden may be defined as a fixed distance between inter blast holes in a different blasting patch row and moving the perpendicular direction to the free face. The valid or effective burden mainly depends on the selection of delay patterns. Many relationships and formulae are available to determine or calculate the approximate burden values. Most connections are utilized basic parameters like charge weight, charge volume, and blast hole diameter.

Anderson (1952) proposed many most straightforward formulae using charge diameter as the independent variable. The relation did not consider either the physical properties of rock mass or explosives properties.

Pearse (1955); Allsman (1960); Speath (1960) were suggested a similar formula to account for the characteristics of explosives and the strength of materials. The difficulty of applying these relationships lies in selecting appropriate values for explosive and rock mass.

Ash (1968) proposed a modified formula to determine the burden dependent on blast hole diameter.

2.6.2 Spacing

Spacing may be defined as a fixed distance between the blast holes in the same row and parallel to the free face. It measures in a perpendicular direction to the burden. Spacing is determined by using the burden, blast hole depth, relative primer location between two adjacent charges, and initiation time interval.

Fraenkel (1957); Speath (1960); Ash and Pearse (1961); Kochanowaski (1963); Lewis and Clark (1964) were established spacing to burden ratio have been used one to two for the excellent fragmentation mostly in mining operations.

Vutukuri and Bhandari (1973) suggested a ratio between spacing and burden is 1.2:1.3 found from field investigation during 100 mining operations that drilled to spacing to burden ratio.

Bhandari (1975) suggested the break angles as much larger up to 150^0 for optimum fragmentation burden, which allowed the spacing to burden ratio to be greater than two. It was also explained to reduce the burden for properly utilizing stress wave energy and gas energy, resulting in improved fragmentation. Recommended spacing to burden ratio is up to 3 or 4 with the reduced burden. The usefulness of laboratory tests result has also been proved in production scale blasting.

2.6.3 Stemming and Decking

The primary purpose of the **stemming** is to return the original condition of the blast hole (i.e. single column charge) by rifling the top portion hole as much as possible, and it helps to reduce noise. Stemming also serves to confine produced gases after the explosion until it is adequate time to fracture and displace rock mass. Stemming and its length significantly impact the stress wave energy after the blast. But it reduced the expansion of the high-

pressure gases into the atmosphere after the explosion. The suitable stemming height enhances fractures and rock mass displacement produced by blasting energy (Bhandari, 1976). Rules of thumb say that stemming is greater than or equal to burden. Similarly, the decking is used in a double-column charge blast hole.

2.6.4 Maximum charge per delay

The maximum amount of explosive is charged to detonate within an applied proper delay detonator, is known as maximum charge per delay or charge weight per delay. It also plays a vital role in the fragmentation of rock mass in mining operations and the generation of ground vibrations. The propagation of ground vibrations depends on the maximum charge per delay.

2.6.5 Explosives

ANFO: the explosive material is one of the most reactive substances that contain a huge amount of potential energy. After the explosion, energy is released as light, heat, sound, and pressure. ANFO (or Ammonium Nitrate/Fuel Oil) is a blasting agent technically but is widely used bulk explosive industrial mixture in mines and quarries operation, and its name is commonly pronounced as "ANN-foe" (Britannica, 2019). It consists of 94 % prilled/porous ammonium nitrate (NH_4NO_3), (AN) that acts as the oxidizing agent and absorbent for the 6 %, number 2 fuel oil (FO), popularly known as High-Speed Diesel (HSD). This forms a reasonably powerful commercial explosive. ANFO is non-cap-sensitive explosives and requires a large shockwave to set it off (Cook, 1974). ANFO has found wide use in coal mining, quarrying, metal mining, and civil construction applications where the advantages of ANFO's low cost and ease of use matter more than the benefits offered by conventional industrial explosives, such as water resistance, high detonation velocity, and performance in small diameters. Globally, this product accounts for an estimated 80% of explosives used annually. To keep the cost down, bulk ANFO is used, i.e., mixed at the mines near the borehole by a bulk truck or stationary mixer (Mathiak, 1965).

Slurry: Slurries are water-resistant explosives based that are pumpable and contained in plastic bags. This type of explosive is designed for wet conditions and used in large blast hole diameters.

Emulsions: the emulsion is a water resistant commercial explosive used in different mines that delivers a high velocity of detonations VOD, that is 5 km/sec to 6 km/sec. The ingredients of the emulsion explosive comprise of the fuels and oxidants that produces high shock wave for rock fragmentation and displacement of rock mass. Here, the ratio of fuel to oxidants elements is 10:1 (Pickering, 1999).

2.6.6 Blast Hole Design

The length and area of the blast hole also play an important role in the proper rock fragmentation and displacement of the rock mass. Single column and double column charge blast holes are used in mining operations depending mainly on the thickness of the rock bed or coal seam. A single-column charge blast hole is smaller in length and explosive-filled by one time. In contrast, a double-column charge hole is larger and explosive-filled by two times separated by proper decking. Blast hole patch prepared to the final stage for blasting in the minefield, as shown in Figures 2.12 and 2.13, respectively.

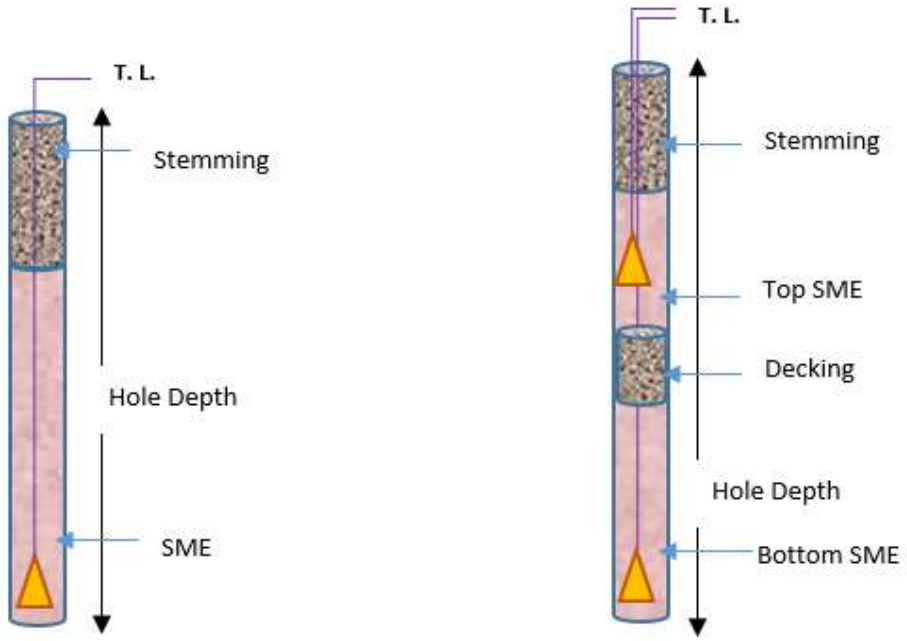

Figure 2.12 Single and double column charged blast hole (Kumar et al. 2021)

Figure 2.13 Preparation of blast holes in a patch

2.6.7 Powder Factor

The powder factor is the relationship or ratio between how much rock mass (tons) is broken and how much explosive (kilogram) is being used to break it.

Gustafsson (1981) suggested that if the length of burden increase by 3m, the rock mass fragmentation becomes uncontrollable, especially at the upper part of the blast hole. At constant burden, the powder factor increase and the average size of fragmentation decrease.

Higher the value of powder factor means a lesser amount of explosive is being used and vice-versa. The powder factor for a single borehole is calculated by the following Equation (2.4)

$$PF = PC*(0.10*\rho)*d^2 / (B*S*H) \quad (2.4)$$

PF: powder factor, pounds of explosives per bank cubic yard of rock

PC: powder column, the meter of explosive charge

ρ: density, kg/m^3, of explosive

d: blast hole diameter

B: burden in meter

S: spacing in meter

H: bench height (hole depth) in meter

2.6.8 Initiation System and Delay Operator

Bhandari et al. (1997) note that an initiation system consists of three basic parts as; an initial energy source; an energy distribution network that conveys energy into individual blast holes; and an in-the-hole component that uses energy from the distribution network to initiate a cap-sensitive explosive. There are two basic initiation systems used in mining operations: electrical and non-electrical.

Smith (1868) introduced a cap that combined a spark gap ignitor and mercury fulminate, the first electric capable of detonating dynamite after the Alfred Nobel (1863).

Smith (1876) and Gardner (1888) developed electric detonators that combined a hot wire detonator with mercury fulminate explosive. These were the first modern-type blasting caps. Modern caps use different explosives and separate primary and secondary explosive changes but are generally similar to the Gardener and Smith cap.

Johansson and Per-Anders Persson (1970) invented a non-electric detonator named 'Nonel' under working Swedish company Nitro Nobel. Today, Nitro Nobel has become a part of Dyno Nobel . Nonel is not affected by any electric hazard is seen as an ideal replacement in

a situation where the electric firing is virtually impossible or not permitted by any agency for one reason or another. Its detonator functions almost like an electric detonator, but the leg wires and fuse head were replaced by the plastic tube through which shock wave transmitted. The end of the shock wave from the plastic tube initiated the delay element in the detonator (Nicholson, 2005). Delay operator is an essential factor used in different surface mining operations to minimize or suppress ground vibration levels and give time intervals to create a new free face. It provides the delay interval between; in-hole blast, hole-hole blast in the same row, inter-row hole blast. The in-hole blast delay operator minimizes the cut-off probability and ensures that all blast holes have been properly primed before the explosion listed in Table 2.1. The hole-hole blast delay operator provides the time interval to create a new second free face between two successive holes through the broken rock mass. Inter-row hole blast delay provides the time interval to create a new second major free face parallel to the initial free face between two successive rows (Bhandari, 1997). A delay detonator and booster was used in the present field and blast hole in the final stage for blasting, as shown in Figure 2.14.

Figure 2.14 Applied delay, booster, and blast holes ready for blasting

Table 2.1: The minimum delay intervals suggested by different researchers

Sl. No.	Researchers	Minimum delay interval between the blast holes
1	Konya (1968)	**3-4ms**: Diabase porphyrites, compact gneisses, mica schist and magnetite rocks mass. **4-5ms**: Compact limestone and marbles, granite and basalt, quartzite gneisses rock mass. **5-6ms**: Some limestone, rock salt, some shale. **6-7ms**: Sandstone, loams, marris, and coal seam.
2	Lang and Favreau (1972)	**5-8ms**: per meter of burden
3	Langefors and Khilstrom (1973)	**2-5ms**: per meter of burden
4	Bergman et, al. (1974)	**3-6ms**: per meter of burden
5	Hagan (1977)	**8ms**: per meter of burden for soft rock mass. **4ms:** per meter of burden for hard rock mass.
6	Winzern (1978)	**11ms**: per meter of relief between blast holes and **28ms** along the echelon.
7	Andrews (1981)	**3-17ms**: per meter of spacing between adjacent blast hole in the same row. The inter rows delay about 2-3times to adjacent hole delay.

2.6.9 Initiation Pattern

In a **square pattern**, spacing and burden have an equal length. The spacing length is larger than the burden length in a **rectangle pattern**, as shown in Figure 2.13. **V-**pattern (chevron or echelon rounds) firing comes under both square and rectangle blasting patterns while not under the staggered blasting pattern. Therefore, the V-pattern firing is used in any square or rectangle blasting operation. The actual burden and spacing (both dependent upon the timing of shot) will differ from the apparent spacing and burden, as shown in Figure 2.15. A **V**-pattern firing round is used in a square-pattern loading scenario, and the rock mass movement is 45^0 to the open fac. **V**-pattern firing rounds are quite common at surface coal mines that use larger diameter blast holes. Echelon patterns are typically designed to take advantage of two free faces; they are typically used in large overburden shots (i.e. in blast holes with diameters greater than 8 inches) casting operation and inter-burden shooting (Hagan, 1986).

Hagan (1986) maintained that blast holes drilled on equilateral triangles patterns produce the best fragmentation in hard rocks. However, weaker rock blasting creates good fragmentation by using rectangular and square patterns.

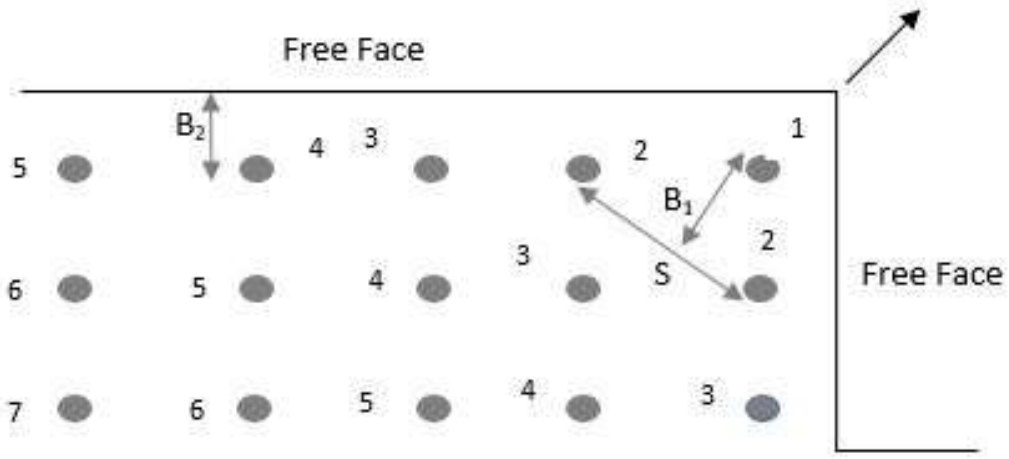

Figure 2.15 Rectangle pattern of blasting patch

In a **staggered pattern,** the drilled spacing of each row is offset such that the holes in one row are positioned in the middle of the spacing of the holes in the preceding row. In addition, the spacing is larger than the burdens. A staggered blasting pattern is used for row firing, where the holes in a row are fired before the holes in the row immediately behind them, as shown in Figure 2.16. The square and rectangle blasting patterns are used for V-pattern firing (i.e. chevron or echelon) (Bhandari, 1975).

Bhandari (1975) suggested that the staggered pattern is more efficient than the rectangular and square pattern and tested at a small scale with staggered holes' toe between holes removed ever when spacing is excessive.

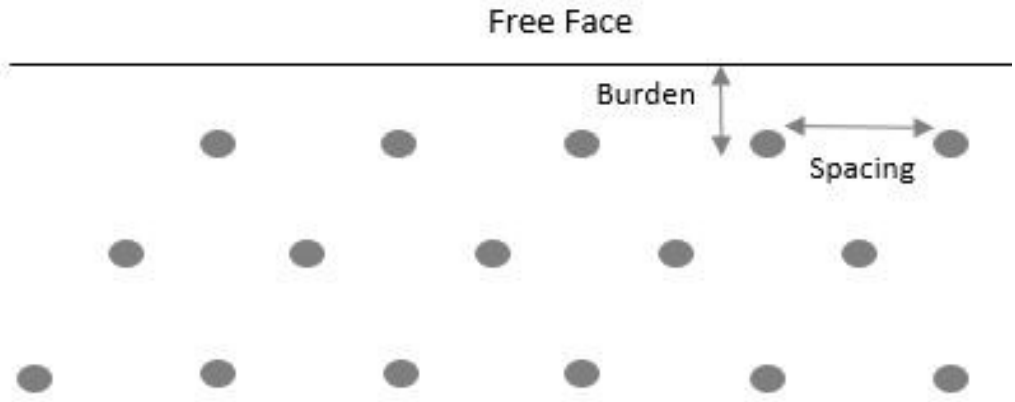

Figure 2.16 Staggered initiation of blasting patch

2.7 Instrument

2.7.1 Seismograph

A seismometer is an instrument that responds to ground noises and shaking such as caused by earthquakes, volcanic eruptions, and explosions. They are usually combined with a timing device and a recording device to form a seismograph (Agnew et al. 2002). The seismograph is used to monitor the parameters in different mine and quarriy listed in Table 2.2. Seismograph recorded the monitored data by geophone and provided the digital information on the device. Data transfer from seismograph into the computer via a particular cable type through software. In the present field, a geophone associated with mini SUPERGRAPH is used to monitor digital data display on its screen, as shown in Figure 2.17. Geophones have historically been passive analogue devices and typically comprise a spring-mounted wire coil moving within the field of a case-mounted permanent magnet to generate an electrical signal. It is susceptible to sound and seismic wave energy to convert mechanical energy into electrical signals (Rynolds, 2011). The modern geophone comprises three orthogonal coils to record the seismic movements in radial, transverse, and vertical velocity directions.

Table 2.2: Details of monitoring Instruments

S.No.	Seismograph	Type and Model	Serial No.
1	Minimate	Instantel	5472
2	Minimate Plus	Instantel	BE10076
3	Minimate Ds-077	Instantel	4537
4	NoMis	Seismograph MSG x2	12595

Figure 2.17 Installation of an instrument in field and acquired digital data

2.8 Recording Parameters

2.8.1 Scaled Distance

The concepts of scale distance are mainly based on the maximum amount of explosive per delay used in a blasting and monitoring distance from the blast site. To derive the Equation (2.5) for scaled distance, using maximum charge per delay and distance.

$$SD = R/\sqrt{Q_{max}} \quad (2.5)$$

Typically, the square root of maximum charge per delay is used in blast-induced ground vibration study and rarely cube root is used. At the same time, the concept of cube root is used in air overpressure study. The wavefront originating from the cylindrical column charge by the ratio of a length to diameter ratio is 6:1 results, the expansion of wavefront as cylindrical form. The volume of the cylinder is directly proportional to the square root of the radius of the cylinder. Thus, the peak level of ground motion at any given point is inversely proportional to the square of the distance from the shot point (OSMRE, 1983). US Office of Surface Mining (OSM) reviewed the criteria proposed by USBM and developed a workable

distance-dependent peak particle velocity (PPV) criteria listed in Table 2.3. These criteria are included in the US Code of Federal Regulations (CFR).

Table 2.3: Maximum allowable peak particle velocity for blasting vibrations (OSME, 1983, 30 CFR, Parts 715, 780, 816, 817).

Distance from blast site (m)	Maximum allowable peak particle velocity (mm/s)	Scaled distance factor to be applied Without seismic monitoring
0-92	31.75	50
92-1524	25.40	55
>1524	19.05	65

2.8.2 Peak Particle Velocity (PPV)

Radial velocity is measured in a horizontal direction toward the propagation of wave parcel, also known as longitudinal velocity.

Transverse velocity is measured in a perpendicular direction in a longitudinal plane toward the propagation of the wave parcel.

Vertical velocity is measured in the mutually perpendicular direction to the radial and transverse plane toward the propagation of the wave parcel.

The propagation velocity radiates seismic waves into a medium and is measured by m/s. The velocity of propagation is different from the particle velocity. As the seismic waves travel through the rock, there are movements of the particles. This is commonly referred to as vibration. The motion of the ground particles (vibration) occurs in three dimensions: vertical, radial, and transverse. When there is vibration, each particle has a velocity, and the maximum velocity among the velocity components is referred to as the peak particle velocity PPV. The intensity of ground vibration is more disturbing or hazardous events. Thus, several scientists and researchers have tried to establish the correlation between the ground vibration parameters (i.e. displacement, velocity, acceleration, and dominant frequency) and human disturbance, damage to Structures (Crandell, 1949; Morris 1950; Duall and Fogelson, 1962; Wiss, 1968; Nichols, 1971; Medearis, 1977; Siskind, 1980; and Dowding, 1996).

Duval-Fogelson (1962), Nichols (1971), and Wiss (1968) suggested that structural damage correlates with the intensity of ground vibrations (PPV). Equation (2.6) represents the predictor model for ground vibration, and it depends mainly on two basic parameters like maximum charge per delay (Q_{max}) and observation distance (D) from the blast site, k and b are the site-specific constants of rock mass.

$$PPV = k*(D/\sqrt{Q_{max}})^{-b} \quad (2.6)$$

Langefors-Kihlstrom (1963) has also suggested the modified empirical predictor equations for ground vibration. These also depend mainly on the maximum charge per delay, observation distance, and two or more than two site-specific constants of the rock mass. Equations may be linear or non-linear, exponential, etc. Some literature is focused on defining the peak particle velocity depending on the types of equipment.

Hiller-Crabb (2000) and Jackson et al. (2008) have established the relationship for the intensity of ground vibration generated by roller drum at a short distance, considering the roller drum length. Hillar-Crabb measured the intensity of the ground vibration during construction using different controlled equipment. Jackson et al. and Hanson et al. provide a national approach to evaluating the ground vibrations generated by construction equipment in the USA.

Based on experimental data, **Dowding (1980)** also proposed the predictor model equation to predict ground vibration hammer impact. However, several machines usually work simultaneously, which is necessary to analyze the overall effect of the ground vibrations.

2.8.3 Peak Vector Sum (PVS)

In general, the empirical observations of cracking have been made with single component peaks; therefore, using the maximum vector sum provides a significant unaccounted safety factor. As a result, peak particle velocity, the maximum particle velocity among the radial,

vertical, and transverse components recorded from the same blast event should be considered instead of the peak vector sum (Dowding, 1985). Peak vector sum (PVS) is a mathematical term and is defined as the square root of the sum of the square of Radial (R), Vertical (V), and Transverse (T) velocity in the following Equation (2.7).

$$PVS = \sqrt{(R^2 + V^2 + T^2)} \quad (2.7)$$

2.8.4 Dominant Frequency

The frequency is one of the most important parameters to evaluate the damage to the structures and human discomfort caused by blast-induced ground vibration. The frequency may be defined by the number of vibrations and oscillations created in one second and based on the velocity and wave wavelength of the Equation (2.8). The same peak particle velocity characteristics are different at different dominant frequencies. Surface structures have their natural frequency under which structures vibrate or oscillate without any effects and damage after vibration attenuation (Erten et al. 2009).

Medearis (1978) suggested that the natural frequency of structures is related to their height and strength and varies from 4-18Hz. When the natural frequency of the structures is close to the frequency of blast-induced ground vibration, a significant amount of ground vibration energy transmits to structures, which results in oscillations at structures, with increasing amplitude. Therefore, the frequency of the measured ground vibrations should be taken into account for the evaluation of structural damage.

Hennelius (1974) stated that the permissible limit of whole building structures usually occurs below 10 Hz. In contrast, the permissible limit of their walls and ceilings occur in the range (10-16Hz). To summarize, the response of building structures to ground vibration is typically having the permissible limit of the whole building structure at about 4Hz o foundation, at about 20-30Hz on floors, and about 40Hz on the walls and windows. The natural frequency

and damping factor of any building structure are known then we calculate the structure's response (Newmark and William, 1982).

$$f = v*\lambda \quad (2.8)$$

2.9 Ground Vibration Damage at Different Level

2.9.1 Human Response

In the last few decades, many studies have been done on the environmental impacts of blast-induced ground vibrations (BIGV), especially for structural damage criteria and some other studies focused on human perception of BIGV. Human bodies' sensitivity to ground vibration and their sensitivity more than ten times greater than the building structures and different people react differently at same BIGV the degrees of perception of human beings are given depending on the duration of vibration (Siskind et al. 1980), as shown in Figure 2.18. The sensitivity of human bodies depends mainly on the peak particle velocity and dominant frequency, event duration and event frequency. A major part of blasting energy is transmitted into the ground, and radiating outward from the source can cause damage to structures. The structures may not undergo damage at peak particle velocity but lie between (10-50mm/s), while the people may be uncomfortable at 2mm/s.

Raina et al. (2004) remarked that the human body responds to ground vibration can be physiological or psychological. Due to a lake of studies on the physiological effects of blasting vibration, they investigated the impact of BIGV on the human brain and have done experimental studies on six different people; one of them is a female candidate at four different ground vibration levels 0.37mm/s, 11.7mm/s, 33.5mm/s, and 48.25 mm/s. Electroencephalogram (EEG) was used in this study to investigate the activity and function of the brain. They found no significant brain response to transitory vibrations. The feeling and observation of ground vibrations and psychological discomfort or disturbance vary from one person to another person. Decorating objects and others may move or vibrate due to

vibration kept within structures (shaking of lamps, movement of trinkets, sounds of other household goods caused by the ground vibrations).

Hendron and Oriard (1972) suggested ground vibration velocity values 0.8mm/s for perceptible and 5mm/s is found to be disturbing.

Raina et al. (2004) followed this suggestion in their study . Humans begin to perceive ground vibration at around 0.762 mm/s of peak particle velocity (PPV). Depending on the activity, sensitivity, and whether or not human subjective tolerance to ground vibration is variable, however, levels of 12.7 mm/s annoy some people. Although complaints can occur at any level perceptible to humans, they are unusual below 2.03 mm/s and so on.

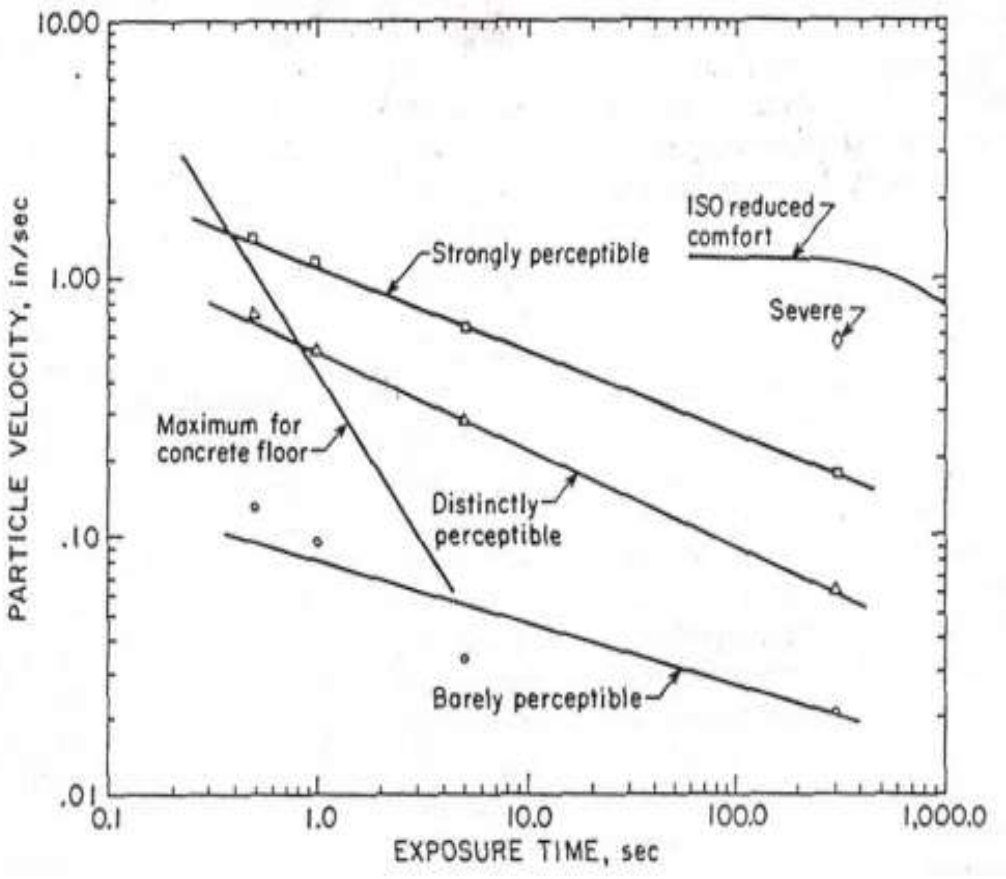

Figure 2.18 Human response to vibrations in a different time (Siskind et al. 1980).

2.9.2 Structural Response

The human being and structural response to annoyance problems from ground vibration are aggravated by wall rattling and other noises. While one of the lowest proposed allowable the ground vibrations for the structures 1.27 mm/s as unacceptable based on direct reactions to the vibrations. Even lower levels cause psychological response problems. Thus, social, economic, and public relations factors become critical for daily blasting. The structures are damaged with cosmetic or hairline, minor and major cracks on with or without plasters walls and roofs due to ground shaking. According to local people, this damages is created by continuous blasting or repetition of ground vibration. Many researchers studied the damage to structures. Generally, the structure's response is classified in the three categories arranged below to increase the distances with declining severity (Dowding, 1992).

- Major (Permanent Distortion). Resulting in severe weakening of the structure (e.g. large cracks or shifting of foundations or bearing walls, major settlement resulting in distortion and weakening of the superstructure, walls out of plump).
- Minor (Displaced Cracks). Surficial, not affecting the strength of the structure (e.g. broken windows, loosened or fallen plaster), hairline cracks in masonry.
- Threshold (Cosmetic Cracking). Opening of old cracks and new plaster cracks, dislodging loose objects (e.g. loose bricks in chimneys) (Dowding, 1992).

2.9.2.1 Induced and Natural Cracking

In control blasting operation, to prevent the threshold and cosmetic cracks and reduces the strain in structures that originate by continuous blast-induced ground vibration and weather changes (Stagg et al. 1984 and Dowding, 1989). The threshold cracks created by continuous induced vibrations can be scientifically observed by visual inspection of the structures continuous, pre and post blasting operation. However, multiple causes of these cracks are considerable in damage analysis to structures. In this consideration, several researchers

(Thoenen and Windes 1942; Anon, 1956; Anon, 1977) noted that they are found to be caused by the following non-blast factors:

- Differential thermal expansion.
- Structural overloading.
- Chemical changes in mortar, bricks, plaster, and stucco.
- It is shrinking and swelling of the wood.
- Fatigue and ageing of wall coverings.
- Differential foundation settlement.

2.10 Standard Damage Criteria

Several damage criteria have been established to enhance blasting efficiency (Duvall et al. 1963; Nicholls et al. 1971; Siskind et al. 1989; Elseman and Rasoul, 2000). Adequate air blast and ground vibration standards have been set by many countries to avoid structural damages and to reduce human complaints. Thus, blasting activities are to be planned and conducted to comply with these standards.

The different countries designed and developed the standard damage criteria limits for different structures based on PPV and associated dominant frequency for the USBM, IS, and German Standard, as shown in Figures 2.19, 2.20, and 2.21. The threshold values of the different structures of different researchers are listed in separate Tables 2.4, 2.5, 2.6, and 2.7, respectively.

2.10.1 United States Bureau of Mine (USBM) Damage Criteria

Table 2.4: USA standard after Siskind et al. (1980) proposed the permissible level of structures.

Type of structures	Peak particle velocity (mm/s)	
	Frequency (< 40 Hz)	Frequency (> 40 Hz)
Modern homes, drywall interior	18.75	50
Older homes, plaster on wood lath construction.	12.50	50

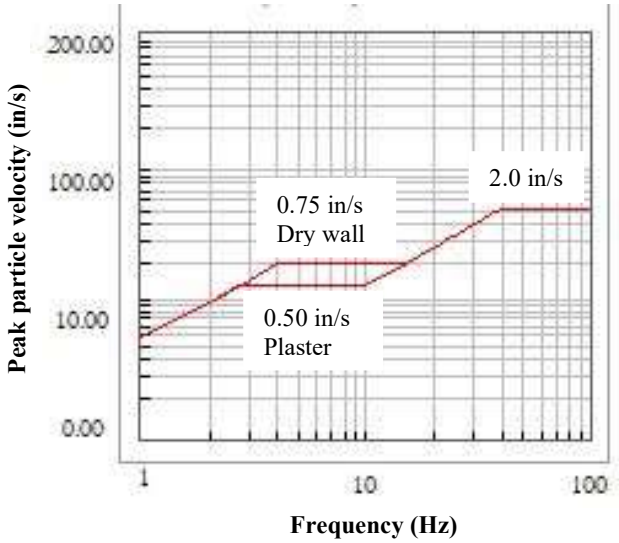

Figure 2.19 Damage criteria for different houses by USBM (Siskind et al. 1980)

2.10.2 Indian Standard (DGMS) Damage Criteria

Table 2.5: Indian standard (DGMS circular 7 of 1997) proposed the permissible level of structures.

Type of structures	Dominant excitation frequency (Hz)		
	< 8 Hz	8-25 Hz	> 25 Hz
(A) Buildings/structures do not belong to the owner			
1. Domestic houses/structures (Kuchcha, Brick and cement)	5	10	15
2. Industrial buildings	10	20	25
3. Objects of historical importance and sensitive structures	2	5	10
(B) Buildings belonging to the owner with a limited span of life			
1. Domestic houses/structures	10	15	25
2. Industrial buildings	15	25	50

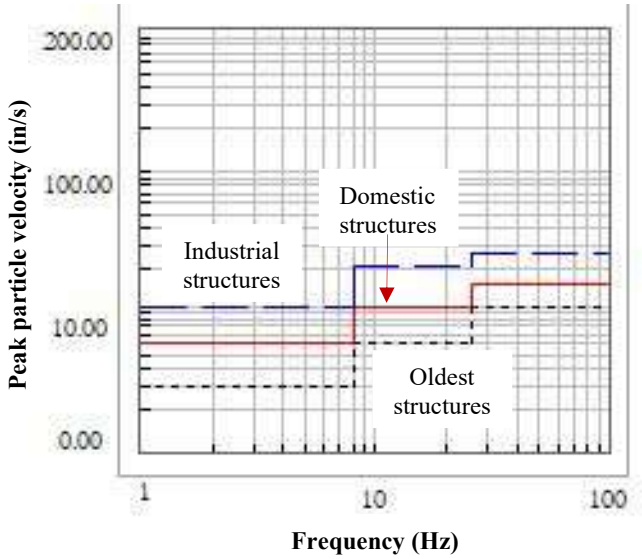

Figure 2.20 Damage criteria for different houses by (IS DGMS, 1997)

2.10.3 German Standard Damage Criteria

Table 2.6: German standard after German (DIN 4150, 1999) proposed the permissible level of structures.

Type of structures	Peak particle velocity (mm/s) at the foundation		
	< 10 Hz	10 -50 Hz	50 -100 Hz
Offices and industrial premises	20	20-40	40-50
Domestic houses and similar constructions	5	5-15	15-20
Buildings that do not come under the above because of their sensitivity to vibration	3	3-8	8-10

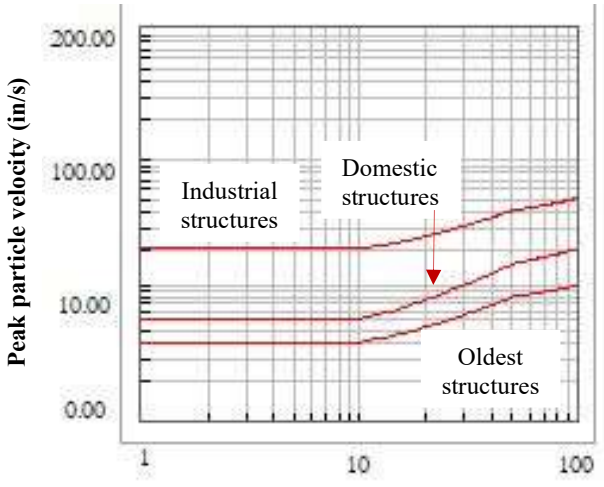

Figure 2.21 Damage criteria for different houses by (DIN 4150, 1999).

2.10.4 Australian Standard Damage Criteria

Table 2.7: Australian Standard 2006 (AS 2187.2) proposed the permissible level of structures (Just and Chitombo, 1987).

Type of structures	Maximum Values
Historical buildings and monuments and building of special value	0.2 mm displacement for frequencies less than 15 Hz
Houses and low rise residential buildings, commercial buildings not included below	19 mm/s resultant PPV for frequency greater than 15 Hz
Commercial buildings and industrial buildings or structures of reinforced concrete or steel construction	0.2 mm maximum displacement corresponds to 12.5 mm/s PPV at 10 Hz and 6.25 mm/s at 5 Hz

2.11 Approaches

2.11.1 Linear Regression Analysis

Regression analysis is a powerful statistical method that examines the relationship between two or more independent variables. Equation (2.9) looks like the equation of a straight line.

$y = \beta_0 + \beta X$ and $y = \log PPV$, $\beta_0 = \log k$, $\beta = (-b)$, and $X = \log SD$ (2.9)

LRA is a suitable mathematical operation to determine the slope and intercept of the straight line equation as site constant. The values of rock mass's site characteristic constant (k, b) are described by above Equations 2.9. It also helps to determine correlation coefficients between measured and predicted values and site-specific constants.

2.11.2 Site-specific Constant

The site-specific constants can be determined by using linear regression analysis. The derived site characteristics constant cannot be applied at different mine and quarry sites because the physical properties of rock mass change from one site to another site.

2.11.3 Empirical Model Equations

In blast-induced ground vibrations study, many scientists and researchers of different countries contributed their efforts. They tried to establish relationships to measure the intensity of ground vibrations. They proposed the different ground vibration predictor models for their countries to optimize the blast design parameters and mitigate the adverse effects of ground vibrations on the structures and natural environments.

2.11.3.1 Duvall-Petkof Model

Assuming cylindrical explosive geometry for long cylindrical charges, Duvall and Petkof, 1959; Duvall and Fogelson, 1962; Duvall et al. 1963; Siskin et al. 1980; Daemen, 1983) of United States Bureau of Mines (USBM), established the fundamental relationships among the peak particle velocity, monitoring distance and the maximum charge per delay. Linear dimension should be scaled to the explosive charge weight's square root based on dimensional analysis. The Equation (2.10) proposed by USBM is.

$$PPV = K[R/\sqrt{Q_{max}}]^{-b} \quad (2.10)$$

2.11.3.2 Langefors-Kihlstrom Model

Langefors et al. (1958), Langefors-Kihlstrom (1963) proposed the following relationships for various charging levels to estimate peak particle velocity and the following Equation (2.11).

$$PPV = K\left[\sqrt{(Q_{max}/R^{2/3})}\right]^{b} \quad (2.11)$$

2.11.3.3 General Predictor Model

Several researchers propose this general empirical Equation (2.12) for vibration prediction (Davies et al. 1964; Attewell, 1964; Birch and Chaffer, 1983; Daemen, 1983). They considered particular charge symmetry.

$$PPV = KR^{-b}(Q_{max})^{A} \quad (2.12)$$

2.11.3.4 Ambraseys-Hendron Model

Ambraseys-Hendron (1968) suggested that any linear dimension should be scaled to the explosive charge weight cube root for spherical geometry. An inverse power law was proposed to relate the amplitude of seismic waves and scaled distance to obtain the following Equation (2.13).

$$PPV = K[R/(Q_{max})^{1/3}]^{-b} \quad (2.13)$$

2.11.3.5 Indian Standard Model

Indian standard (1973) suggested that the blast should be scaled to the equivalent distance or the scaled distance, defined as the explosive charge weight divided by the cube root of the square of real distance. The proposed Equation (2.14)

$$v = K\,[(Q_{max}/R^{2/3})]^{b} \quad (2.14)$$

2.11.3.6 Ghosh-Demon Model

Ghosh–Daemon predictor (1983) proposed that various inelastic effects cause energy losses during wave propagation in various mediums. This inelastic effect leads to a decrease in amplitude and those due to geometrical spreading. They modified the propagation relations of USBM in terms of adding inelastic attenuation factor (α). The following Equations (2.15 and 2.16).

$$PPV = K[R/\sqrt{Q_{max}}]^{-B}e^{-Ar} \quad (2.15)$$

$$PPV = K[R/(Q_{max})^{1/3}]^{-B}e^{-\alpha R} \quad (2.16)$$

2.11.3.7 CMRI Predictor

Roy (1993) proposed a new predictor equation based on the data collected from different Indian geo-mining conditions. This Equation (2.17) is only valid in the zone of disturbance, i.e. when $Q_{max}>0$ and $v>0$.

$$PPV= n+K[R/\sqrt{Q_{max}}]^{-1} \quad (2.17)$$

PPV= peak particle velocity (mm/s)

R = distance between blast face and monitoring point (m)

Q_{max} = Maximum explosive charge used per delay (kg), and

K, A, b, and α = Site constants which can be determined by multiple regression analysis

n = site constants which are influenced by rock properties and geometrical discontinuities

2.11.4 Multivariate Regression Analysis

When the dependent variable depends on more than one independent variable called multi-variable regression analysis (MVRA), which gives its correlation. The general relationship (2.18) is given as:

$$Y = \beta_0 + \beta_1 X_1 + \beta_2 X_2 + \beta_3 X_3 + \beta_4 X_4 + \beta_5 X_5 + \ldots\ldots + \beta_5 X_5 + E \quad \ldots. \quad (2.18)$$

Where, β_0 - intercept and $\beta_1, \beta_2, \beta_3, \beta_4, \beta_5, \beta_n$. are the coefficient or slope of the independent variables $X_1, X_2, X_3, X_4, X_5, \ldots\ldots X_n$ respectively, and error E. Using the MVRA establish the new relationship among the PPV (dependent variable) and independent variables such as; total charge, distance, burden, spacing, no. of holes, hole depth, hole diameter, and total booster, etc. The coefficient of determination (R^2) is usually used to test the predictive ability of a multiple regression equation. A closer value of R^2 to unity implies an accurate predictive model. The multiple regression presents two overlaps: the overlap for the combined effect and the overlap for the individual effect (Enayatollahi et al. 2014).

2.11.5 Fundamental of Artificial Neural Network

The artificial neural network is an information processing system simulating the structure and functions of the human brain. It is a highly interconnected structure that consists of many simple processing elements (called neurons) capable of performing massive parallel computation data processing and knowledge representation. The neural network is first trained by processing many input patterns and the corresponding output. A particular ANN

has three fundamental components; transfer function, network architecture and learning law (Simpson, 1990).

Neural Network ⟹ Artificial Neural Network

(Brain) (Machine)

Hecht-Nielsen (1990) proposed the definition of ANN *as "An Artificial Neural Network is a parallel, distributed information processing structure consisting of* ***processing units*** *(which can possess a local memory and can carry out localized information processing operations) interconnected via unidirectional signal channels called* ***connections****. Each processing unit has a single output connection that branches ("fans out") into as many collateral connections as desired; each carries the same signal -* ***the processing unit output signal****. The processing unit output signal can be of any mathematical type desired. The information processing that goes on within each processing unit can be defined arbitrarily with the restriction that it must be completely local; that is, it must depend only on the current values of the input signals arriving at the processing element via impinging connections and on values stored in the processing unit's local memory."*

Zurada (1998) proposes the following analogy to clarify this point. An ANN being trained using supervised learning corresponds to a student learning by answering the questions posed by the teacher and comparing his answers to the correct answers given by the teacher. The unsupervised learning case corresponds to the student learning the subject from a videotaped lecture provided by the teacher, but the teacher is not available to answer any questions. The teacher offers the methods (the learning rule) and questions (the input training vectors) but not the answers to the questions (the output training vectors).

Anderson and Rosenfeld (1988) have edited a fascinating book that contains a collection of several classical papers in the ANN area.

Nilsson (1965) has published a theoretical view of the state of the field in the mid-'60s.

Lippmann (1987) and, more recently, **Hush and Horne (1993)** published updated reviews of several ANN models.

Simpson (1990) has published an extensive compilation of ANN models.

White (1989) and **Levin et al. (1990)** provide a statistical interpretation of the methods used to train feed-forward ANNs.

Nerrand et al. (1993) show that ANNs can be considered general non-linear filters that can be trained adaptively. They also show that several algorithms used in linear and non-linear adaptive filtering can be seen as special cases of algorithms used to train ANNs.

Frank Rosenblatt (**1958)** proposed the *Perceptron* model in 1958 and 1962 that can also be used as a pattern associator or pattern classifier. The single-layer perceptron model consists of one layer of input binary units and one layer of binary output units. There are no hidden layers, and therefore there is only one layer of adjustable weights. The output units use a hard-limiting threshold output function.

The way to overcome the limitation of linear reparability is to use multi-layer networks, such as the so-called *Multi-Layer Perceptron* (MLP) that introduce extra layers of units (the so-called hidden units) between the input and output layers.

Minsky and Papert (1969) *The perceptron has shown itself worthy of study despite (and even because of!) its severe limitations. It has many features to attract attention: its linearity; its intriguing learning theorem; its clear paradigmatic simplicity as a kind of parallel computation. There is no reason to suppose that these virtues carry over to the many-layered versions. Nevertheless, we consider it a significant research problem to elucidate (or reject) our intuitive judgement that the extension is sterile. Perhaps some powerful convergence theorem will be discovered, or some profound reason for the failure to produce an interesting "learning theorem" for the multi-layered machine will be found."*

Rosenblatt also came very close to discovering the key to training multi-layer perceptron when he proposed a *heuristic* algorithm to adapt both layers of weights

Rosenblatt (1962) states that *"The procedure to be described here is called the "back-propagating error correction procedure" since it takes its cue from the error of the Runits (the output units), propagating corrections back towards the sensory end of the network (the input units) if it fails to make a satisfactory correction quickly at the response end (output units). The actual correction procedure for the connections to a given unit, whether it is an A-unit (hidden unit) or an R-unit (output unit) is perfectly identical to the correction procedure employed for an elementary perceptron (the single-layer perceptron), based on the error-indication assigned to the terminal unit."*

Enayatollahi et al. (2014) made a comparison between Neural Networks and Multiple Regression Analysis to Predict Rock Fragmentation in Open-Pit Mines. It was concluded that the ANN results possess a greater degree of accuracy, are robust, and are more fault-tolerant than any other analysis technique.

2.11.5.1 Neural Network Training

A network first needs to be trained before interpreting new information. A number of algorithms are available for the training of neural networks. Still, the back-propagation algorithm is the most versatile and robust technique and its flow chart is shown in Figure 2.22. It provides the most efficient learning procedure for multi-layer neural networks. Also, the fact that back-propagation algorithms are especially capable of solving predictive problems makes them so popular. He discovered the back-propagation algorithm while working on his doctoral thesis in statistics and called it *the dynamical feedback algorithm*.

Parker (1982) rediscovered the back-propagation algorithm in 1982 and called it *the learning logic algorithm*. Finally, **Rumelhart, Hinton and Williams (1986)** rediscovered the algorithm, and the technique became widely known. Today, the back-propagation

algorithm is the most popular supervised learning rule to train feed-forward multi-layered ANN. Most scholarly articles applied an ANN, particularly the feed-forward back-propagation neural network (BPNN), for the prediction of blast-induced ground vibrations (Saadat, et ak. 2014; Das, et al. 2019; Lawal and Idris, 2019; Rajabi and Vafaee, 2020; Yan, et al. 2020). BPNN is a strong modelling technique for input/output pattern identification problems and is a commonly used ANN, often applied to solve nonlinear problems. The connection weights and bias values are adjusted by gradient descent algorithms. The weights of the interneuron connections are adjusted according to the difference between the predicted and the actual network outputs (Yan, et al. 2020).

The back-propagation neural network consists of at least three layers: input, hidden, and output. Each layer consists of many elementary processing units called neurons.

- Each neuron is weighted and connected to the next layer so that neurons in the input layer communicate their output as input to neurons in the hidden layer.
- It forward passes here output is compared with the measured value.
- The difference of error between both is called bias which proceeds through the network (backward pass), updating the individual weight of the connection and also biases of individual neurons.
- All the neurons in the back-propagation neural are associated with a bias neuron and a transfer function (linear).
- This process is repeated for all training pairs in the data till the network error reaches a minimum threshold value defined by a cost function; usually, the root means squared (RMSE) or summed squared error (SSE) (Khandelwal, 2002).

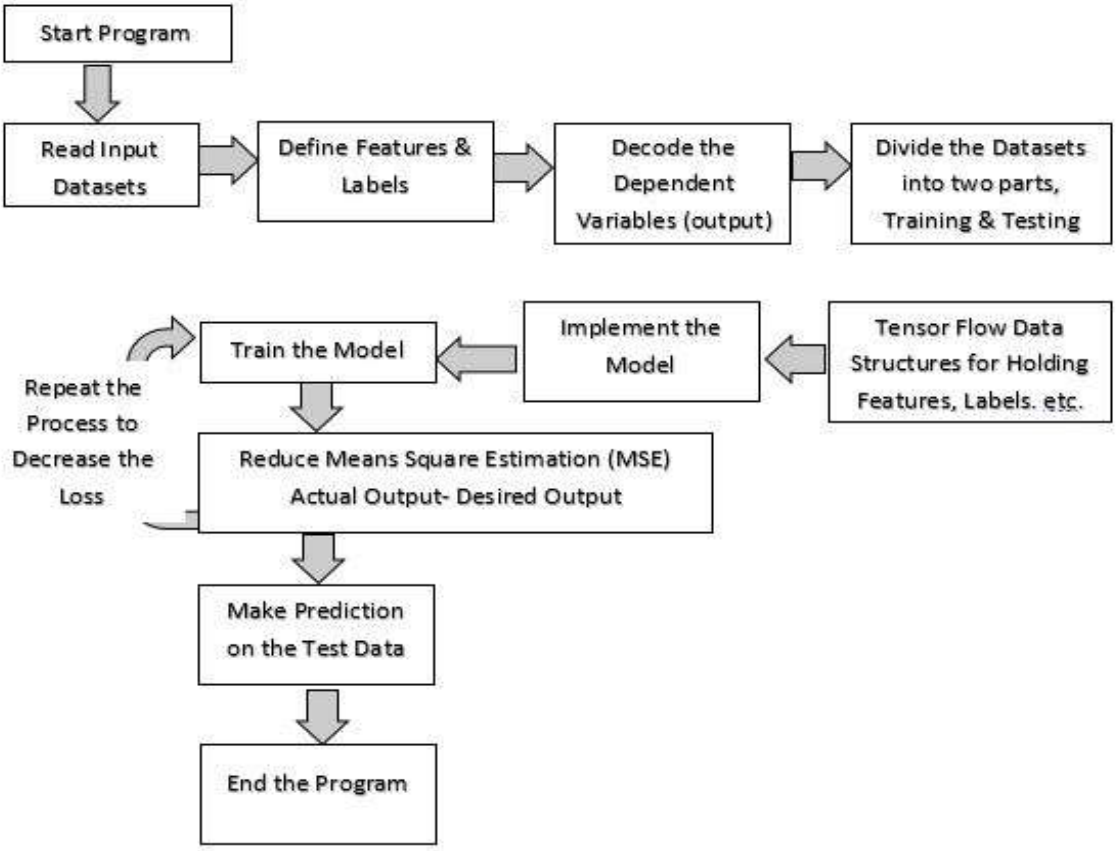

Figure 2.22 Flow chart of BPANN technique from beginning to end of the program

Recently, the back-propagation artificial neural network (BPAAN) technique has become a popular algorithm for analysis and prediction. The construction of the predicted equation for n^{th} input layers is in the following ways:

J^{th} neurons are connected with many inputs as

$X_i = X_1, X_2, X_3 \ldots\ldots X_n$

The net input values in the hidden layer will be

$$Net_j = \sum x_j w_{jk} + \theta_j$$

Where X_i is the input units, w_{ij} are the weights on the connection of i^{th} input and j^{th} neurons, θ_j is the bias neuron(optional), and **n** is the number of input units. The net output from the hidden layer is calculated using a logarithmic sigmoid function of equation (2.19).

$$O_j = f(Net_j) = 1/[1+e^{-(Net_j+\theta_j)}] \quad (2.19)$$

The total input to the k^{th} unit is

$$Net_k = \sum W_{jk}O_j+\theta_k \quad (2.20)$$

Where θ_k is the bias neuron, and w_{jk} is the weight between the j^{th} and the k^{th} output. So the total output from k^{th} unit will be

$$O_k = (Net_k)$$

The error e_l at any output in layer **k** is

$$e_l = t_k - o_k$$

Where t_k is the desired output and o_k is the actual output.

The total error function is given by

$$E= \tfrac{1}{2}\sum (t_k - o_k)^2 \quad (2.21)$$

Training the network is a process of arriving at an optimum weight space for the network. The steepest descent error surface is made using the following rule:

$$\Delta W_{jk} = - \eta (\delta E/\delta W_{jk})$$

Where η is the learning rate parameter, and E is the error function. The update of weights for the $(n+1)^{th}$ is given as

$$W_{jk}(n+1) = W_{jk}(n)+ \Delta W_{jk}(n) \quad (2.22)$$

Similar logic applies to the hidden and output layers. This procedure is repeated with each pair of training cases. Each pass through all the training patterns is called a cycle or epoch. The process is repeated as many epochs as needed until the error is within the user-specified goal (Khandelwal, 2002).

2.11.5.2 Neural Network Architecture

A feed-forward network is adopted here as this architecture is suitable for the problem based on problem identification. Recent works on PPV prediction using soft computation techniques are listed in Table 2.8 (Trigueros et al. 2017). Pattern match is an input and output mapping problem. Closer the mapping better the performance of the network and the architecture of n^{th} layer of feed-forward back propagation technique and its circuit diagram as shown in Figures 2.23 and 2.24. The nomenclature of network architecture follows:

- Number of input neurons
- Number of output neurons
- Number of hidden layers
- Number of hidden neurons
- Number of training epochs
- Number of training datasets
- Number of testing datasets
- Error goal

Other types of ANN applied in the prediction of blast-induced ground vibrations include GRNN, quantile regression neural network (QRNN), wavelet neural network (WNN), hybrid neural fuzzy inference system (HYFIS), adaptive neuro-fuzzy inference system (ANFIS), and group method of data handling (GMDH) (Arthur et al. 2019).

To overcome the limitations associated with ANN in predicting blast-induced ground vibrations, studies have also applied other ML algorithms that are without these shortcomings. Some of the algorithms applied included SVM (Temeng, et al. 2021), particle swarm optimization (Hasanipanah, et al. 2017; Shahnazar, et al. 2017), Gaussian process regression (Arthur, et al. 2020), classification and regression trees, chi-square automatic interaction detection, random forest (Zhou, et al. 2020; Zhang, et al. 2020), hybrid artificial

bee colony algorithm (Taheri, et al. 2016), fuzzy Delphi method and hybrid ANN-based systems (Huang, et al. 2020), cuckoo search algorithm (Fouladgar, etal. 2020), extreme learning machine (Arthur, et al. 2020), and the firefly algorithm (Bayat, et al. 2020; Shang, et al. 2020; Chen, et al. 2021).

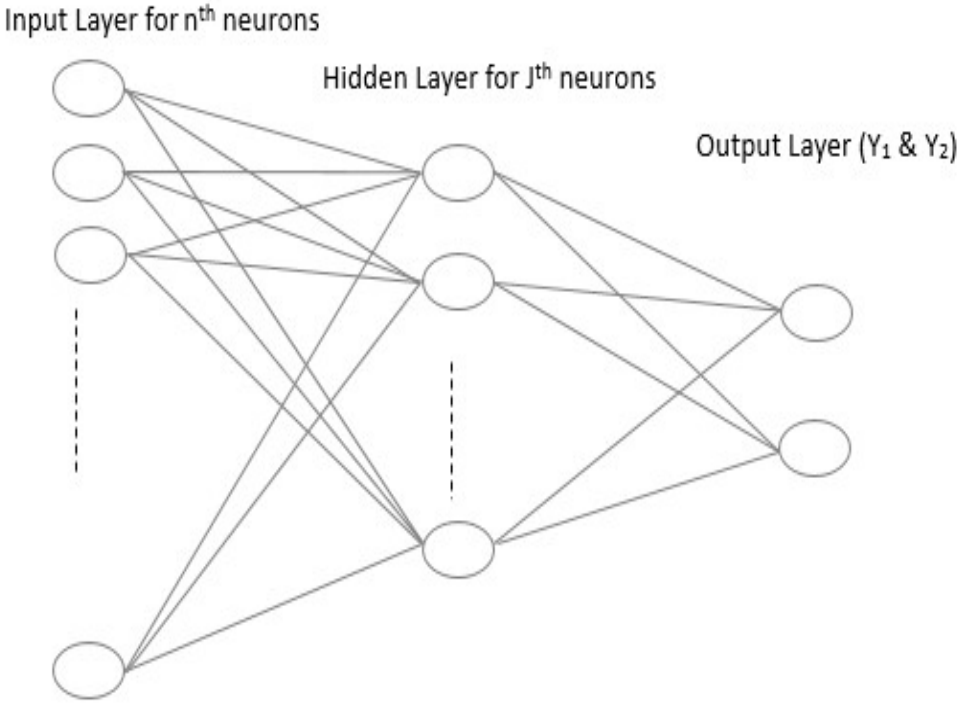

Figure 2.23 The architecture of n^{th} layer of backpropagation ANN technique

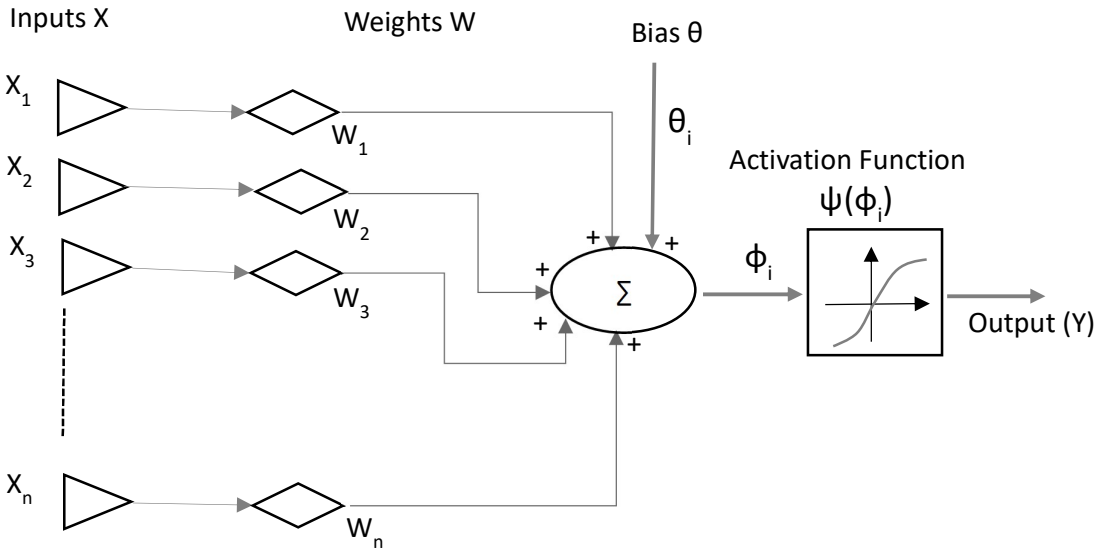

Figure 2.24 Circuit diagram of backpropagation ANN technique

Table 2.8: Recent works on PPV prediction using soft computation techniques.

Sl. No.	References	Algorithm	Input Parameters	No. of Datasets	Correlation Coefficient (R^2)
1	Khandelwal and Singh (2009)	ANN	BI, S, B, HD, D, VOD, Vp, E, υ, C	154	0.98
2	Monjezi *et al.,* (2010)	ANN	BS, N, D, UCS, C, DPR	269	0.95
3	Monjezi *et al.,* (2011)	ANN	HD, ST, D, C	182	0.95
4	Khandelwal *et al.,* (2011)	ANN	D, C	130	0.92
5	Mohamed, (2011)	ANN, FIS	D, C	162	(R^2_{ANN})= 0.94 (R^2_{FIS})= 0.90
6	Fisne *et al.* (2011)	FIS	D, C	30	0.92
7	Li *et al.,* (2012)	SVM	D, C	32	0.89
8	Mohamadnejad *et al.,* (2012)	ANN, SVM	D, C	37	(R^2_{ANN})= 0.89 (R^2_{SVM})=0.85
9	Ghasemi *et al.* (2013)	FIS	B, S, ST, N, C, D	120	0.95
10	Monjezi *et al.,* (2013a)	ANN	C, D. TC	20	0.93
11	Jahed Armaghani *et al.* (2014)	ANN-PSO	HD, S, B, ST, PF, C, DI, N, RD, SD	44	0.94
12	Hajihassani *et al.,* (2015)	ANN-ICA	BS, D, C, ST, Vp, E	95	0.98

Spacing (S); burden (B); stemming (ST); powder factor (PF); specific drilling (SD); support vector machine (SVM); charge per delay (C); hole diameter (DI); hole depth (HD); rock density (RD); number of row (N); particle swarm optimization (PSO); sub-drilling (SD); distance from the blasting face (D); total charge (TC); blastability index (BI); velocity of detonation of explosive (VOD); p-wave (Vp); Young's modulus (E); poison's ratio(υ); burden to spacing ration (BS); delay per rows (DPR); imperialist competitive algorithm (ICA).